Voltage Stability Analysis in Microgrids System with Photovoltaic Solar Energy under Uncertainty of Loads Variation

Yuttana Kongjeen[1], Weerayut Eiampong[1], Krittidet Buayai[2,*], and Kaan Kerdchuen[1]

ARTICLE INFO

Article history:
Received: 26 July 2021
Revised: 29 September 2021
Accepted: 16 November 2021

Keywords:
FVSI
MCS
Non-linear power flow
Photovoltaic solar energy
Probabilistic power flow

ABSTRACT

This paper presents voltage stability analysis for microgrid systems connected with photovoltaic solar energy (PVSE) and load variation conditions. Non-linear power flow is used to solve a probabilistic load flow (PLF) with Monte Carlo simulation (MCS). The PLF was adapted to solve the voltage stability indices (VSIs) in balanced power flow. Fast voltage stability index (FVSI) was selected to investigate the voltage stability analysis in line VSIs. The IEEE 33 bus radial distribution system was selected to integrate the PVSE and electrical uncertainty load used to solve the VSIs. The results showed that the FVSI from the MCS varied from the uncertainty load, growth rate and PVSE. The FVSI was found to have a weak point in the transmission line. However, the installed PVSE could improve the FVSI of the grid and increase the stability index margin. Therefore, the optimal condition of PVSE and the uncertainty load need to be considered and managed in the future.

1. INTRODUCTION

Modern electrical loads of electrical power systems are becoming a key point to manage. Because of the rapid growth, modern electrical loads are integrated into the grid. They un-predictive the load characteristics when consuming the energy are needed to an optimal energy provider [1]. Uncertainty load models are presented to be studied for solving the load variation of the network and optimal control for increasing the system stability.

In recent years, researchers have studied the probabilistic method applied to a power system that is widely used to solve the electrical power system problem. Renewable energy sources (REs) are widely integrated into the grid that is presented in a benefit and clean energy [2]. The REs can reduce the impact from high penetration level from the electrical loads from the grid under uncertainty load. However, the REs need to be optimally controlled and managed in the best condition of the operation. The study of optimal power flow under generated wind power was applied in a probabilistic interval optimization (PIO) model with profit and risk under the uncertain wind power that revealed the effectiveness of the PIO [3]. It can show the results in a trade-off condition only. Meanwhile, Quasi-Monte Carlo (QMC) simulation is adapted to solve the uncertainty of the wind power using the probability load flow (PLF) and compared it with Monte Carlo simulation (MCS) [4]. It is analyzed by using statistical indices of voltage stability margin that presented QMC the superiority compared to the PLF. The impact of the uncertain load is related to voltage profiles, total power loss and system loading [5, 6]. The voltage stability analysis (VSA) is a major to analyze the voltage stability margin of the microgrid to control and maintain a safety margin. Several researchers indicate that repetition performance is related to voltage stability indices (VSIs) to solve the load installed to the grid. The VSIs consist of Bus VSIs, Overall VSIs and Line VSIs, respectively [7, 8]. The role of the VSA is a key factor of the system operation, which is a condition of system stability. Therefore, the uncertainty of the loads can be represented in terms of the probabilistic load. The PLF was adapted to solve the problem from the proposed voltage stability analysis [9,10]. Photovoltaic solar energy (PVSE) is one type of the REs that produces electrical energy and is integrated into the microgrid in this study. Therefore, reducing the variable to find the weak point of the electrical power system is important to find for increasing the reliability of grids. This paper aims to solve the voltage stability analysis by using the fast voltage stability index (FVSI). The FVSI is selected to solve the voltage collapse stability level from the uncertainty load and installed PVSE in the radial distribution system.

[1]*Department of Electrical Engineering, Faculty of Engineering and Architecture, Rajamangala University of Technology Isan, 744 Suranarai Rd., Nai-Muang, Muang, Nakhon Ratchasima, 30000, Thailand.*
[2]*Intelligent Power System and Energy Research (IPER), Department of Electrical Engineering, Faculty of Engineering and Architecture, Rajamangala University of Technology Isan, 744 Suranarai Rd., Nai-Muang, Muang, Nakhon Ratchasima, 30000, Thailand.*
**Corresponding author:* Krittidet Buayai; Tel: +66-8-1916-5989; e-mail: kittavit.bu@rmuti.ac.th.

This paper is organized as follows: problem formulation is explained in section 2, section 3 propose the approach and case study by showing, section 4 the simulation results. Finally, the conclusion and future work are presented in section 4.

2. PROBLEM FORMULATION

2.1 Fast voltage stability index (FVSI)

The FVSI is a type of voltage stability index used to solve the line stability index in a static and dynamic power flow of the grid. The FVSI is adapted to predict the critical transmission lines' voltage collapse point and contingency ranking [7]. The effect of load variations is a direct impact on transmission line systems. The FVSI is presented in Fig.1.

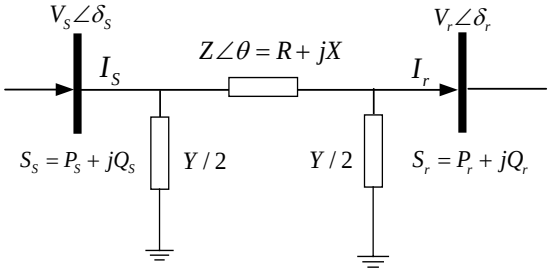

Fig. 1. The two bus equivalent circuits of the power system.

Fig.1 shows the equivalent circuit of the power system, which is used to solve the concept of the VSA. It is related to the power flow between the sending nodes to the receiving node throughout the power transmission line. This concept was brought to adapt the VSA in each methodology. However, the fast voltage stability index (FVSI) was selected to analyze the purpose of the VSA under integrated solar power system and load variant conditions. The FVSI is must be below 1 to indicate a stable transmission line and can be expressed as follows [7].

$$FVSI\left(mcs\right) = \frac{4Z^2Q_r}{V_s^2X} \tag{1}$$

where S_s and S_r are apparent power at the sending and receiving buses, respectively; P_s and Q_s are active and reactive power at the sending bus; P_r and Q_r are active and reactive power at the receiving bus; V_s and V_r are voltage magnitude at the sending and receiving buses, respectively; Y is line shunt admittance; R, X and θ are line resistance, line reactance and line impedance angle, respectively. mcs is iteration period of the Montre Carlo simulation (MCS).

2.2 A nonlinear power flow analysis (NPFA)

NPFA was adapted to solve the power flow problem of the power system. Especially, microgrid systems have a crucial point in an analysis of the problem of instability conditions. The importance of the NPFA is that it can compute the power flow component as voltage profiles, power flow and current of the unbalanced network. Moreover, the modern loads are integrated into the grid with the power consumption's uncertainty level. The modern loads affected the grids in real-time monitoring. Nodal analysis is used for current injection concerning the voltage level of the node. The nodal analysis can be expressed from the OpenDSS program as follows [11]:

$$I_{inj}\left(V\right) = Y_{system}V \tag{2}$$

where, $I_{inj}(V)$ is injection currents from power conversion (PC) elements in the grid; Y_{system} is admittance value of the grids. Therefore, the voltages of the nodes were computed by Eq. (3) as follows:

$$V_{n+1} = \left[Y_{system}\right]^{-1} I_{inj}\left(V_n\right) \quad n \in 0,1,2,...until converged \tag{3}$$

2.3 Monte Carlo simulation (MCS)

MCS was adapted to generate the load variation based on a stochastic programming method. The normal distribution function generates the grid's uncertainty load [3, 5]. Constant power load is defined as an uncertainty load that is related to active and reactive power components. Therefore, the uncertainty load can be expressed as follows [12]:

$$P_{L_i}\left(mcs\left|\mu_{P_{L_i}},\sigma_{P_{L_i}}\right.\right) = f_{P_{L_i}}^{-1}\left('Normal', mu\left(mcs\right), \mu_{P_{L_i}}, \sigma_{P_{Li}}\right) \tag{4}$$

$$Q_{L_i}\left(mcs\left|\mu_{Q_{L_i}},\sigma_{Q_{L_i}}\right.\right) = f_{Q_{L_i}}^{-1}\left('Normal', mu\left(mcs\right), \mu_{Q_{L_i}}, \sigma_{Q_{Li}}\right) \tag{5}$$

where, $\mu_{P_{L_i}}, \sigma_{P_{L_i}}$ are represented mean and standard deviation of the active power of i^{th} the load. $\mu_{Q_{L_i}}, \sigma_{Q_{L_i}}$ are represented mean and standard deviation of reactive power of i^{th} the load; mu is represented by the uniform random number.

2.4 Photovoltaic solar energy (PVSE)

PVSE is one type of the distributed generator (DG) that have many different power sources. The DG types can be classified into four types: injected reactive power, injected real and reactive power, injected real and reactive power, and consumed reactive power but inject real power, respectively. Therefore, this study applied DG type using the injected real and reactive power in the balance of injected power when installing and generating active power with constant power factor only [13]. The PVSE can be expressed as follows.

$$P_{PVSE} = S_{PVSE} \times \cos\theta_{PVSE} \tag{6}$$

where, S_{PVSE} is represented the apparent power of the photovoltaic source; $\cos\theta_{PVSE}$ is represented the power factor of the photovoltaic source.

2.5 Total real power loss

Real power loss (RPL) of the grid is a critical factor in real situations' uncertainty load. The RPL can be computed using the apparent power through the transmission line as Eq. (7)[14].

$$P_{Loss} = \sum_{k=1}^{n} \left(I_k^2 \times R_k \right) \quad (7)$$

where, R_k is the resistance of the transmission line *k*; I_k is the current flow of the transmission line *k*; *n* is number of the transmission line.

2.6 Best hit generation index (BHGI)

BHGI is used to evaluate the frequency of the weak point of the transmission line when loading variation by using the FVSI. The maximum value of the FVSI of the transmission lines in the power system is indicated by counting the number of the BHGI with the transmission line number. Therefore, the PLF from the MCS presented the number of the BHGI generations and occurred the weakness point of the transmission line. This methodology can verify the robustness of the power system from the load variation level. The BHGI can expressed in Eq. (8) as follows:

$$BHGI = \sum_{i=1}^{MCS} Max\left(L_{(k,i)} \in \begin{cases} 1 = Max\left(FVSI_{(k,i)}\right) \\ 0 = Otherise \end{cases} \right); k = 1...m \quad (8)$$

where, *L* is the transmission line number (*k*); *i* is iteration number of MCS; *m* is total of the transmission line number.

3. PROPOSED APPROACH AND CASE STUDY

The microgrid system is selected using the IEEE 33 bus with the radial distribution system and applied to analyze the VSA based on the probabilistic load flow (PLF) presented in Fig.2. The purpose of the FVSI was applied in the static power flow condition. The total real power loss and energy demand were considered to analyze the simulation results. The IEEE 33 bus radial distribution system consists of 32 transmission lines, total loads connected to 3.715 MW and 2.300 MVar [15]. Meanwhile, the total losses as presented by active power and reactive power are 202.46 kW and 130.15 kVar, respectively [16]. The uncertainty load profiles of the grid were implemented by Eq.(4) and (5). The power rates of PVSE was defined by a 0.5 MW and power factor of 0.98. in a static state condition on a peak power generation[8]. The MCS iteration is defined by 1,000 iterations of each case of the PLF. The $\mu_{P_{Li}}$ and $\mu_{Q_{Li}}$ are defined by using load data connected from the system. Meanwhile, the $\sigma_{P_{Li}}$ and $\sigma_{Q_{Li}}$ are defined by using 31.25 % of the standard deviation of the load data connected from the system.

The growth rate of the load was used to solve the high-level impact of the uncertainty load. Therefore, the study cases are divided into 8 cases for analyzing the uncertainty load and defined the growth rate at 1% and 1.5% variation of the FVSI as follows:

Case I: - Only electrical load installed with growth rate = 1
Case II: -Electrical load and PVSE installed bus No.6 with growth rate = 1
Case III: -Electrical load and PVSE installed bus No.18 with growth rate = 1
Case IV: -Electrical load and PVSE installed bus No.33 with growth rate = 1
Case V: -Only electrical load installed with growth rate = 1.5
Case VI: -Electrical load and PVSE installed bus No.6 with growth rate = 1.5
Case VII: -Electrical load and PVSE installed bus No.18 with growth rate = 1.5
Case VIII: -Electrical load and PVSE installed bus No.33 with growth rate = 1.5

The growth rate of loads is defined by a constant value that is related to the system loading. The growth rate changes are directly affecting the grids loading.

4. SIMULATION RESULTS

Fig.3 shows the number of the BHGI from the MCS process, and the FVSI revealed the maximum voltage collapse from each iteration by showing the most of the BGHI on lines No.2 and No.5, respectively. The installation of the PVSE can reduce the BGHI of the grids and transfer them to the other transmission lines. This can be considered to be a significant step forward in the voltage collapse of the transmission line under the FVSI. Therefore, the FVSI level was presented by uncertainty loads and installed the PVSE.

Fig.4 shows the percentage of BHGI of the MCS process. The number record of the weak point from the BHGI is converted to the percentage that the best hit of the BHGI can represent. Therefore, the simulation results are indicated the weak point of the transmission line No.5 and No.2 that showed by ranking from the highest of BHGI of the grids under uncertainty loads. The load growth of 1 indicated the average of 48.05% in the line No.2, the average of 51.70% in line No.5 and an average of 0.25% in line No.27. Meanwhile, the growth rate of 1.5 indicated the average of 16.43% in line No.2, 83.13% in line No.5 and an average of 0.45% in line No.27. Therefore, the best hit generation of the FVSI was presented by transmission line No.5 weakness point of the network. This work is novel in using the FVSI for solving the uncertainty load and integrated the PVSE.

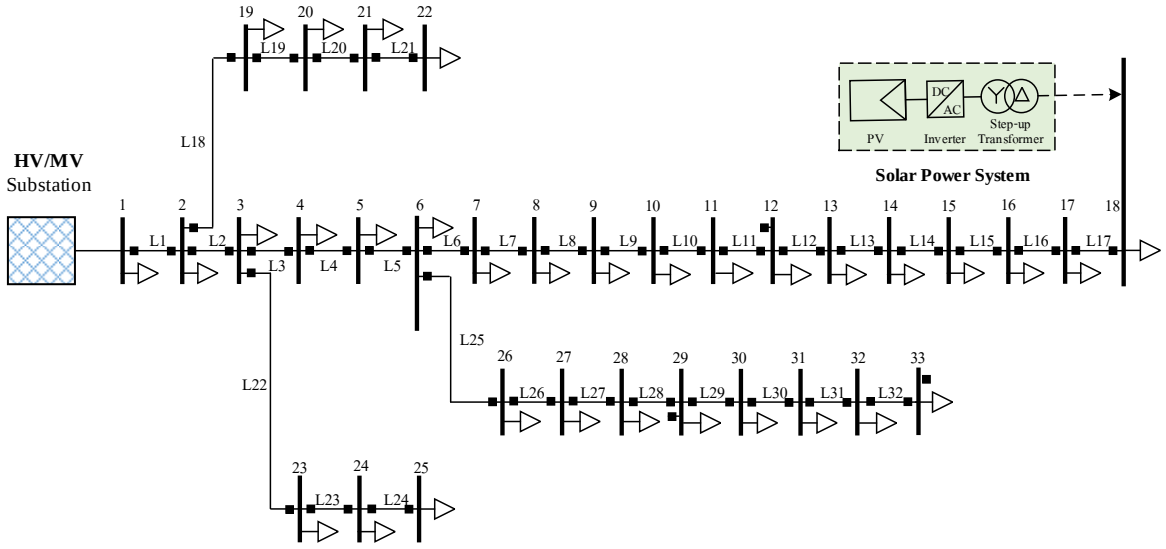

Fig. 2. The IEEE 33 bus radial distribution system under uncertainty load and installed PVSE

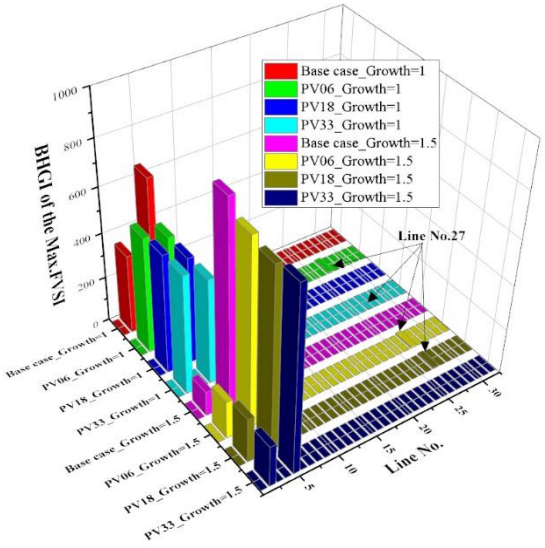

Fig. 3. BHGI results of the maximum value of the FVSI.

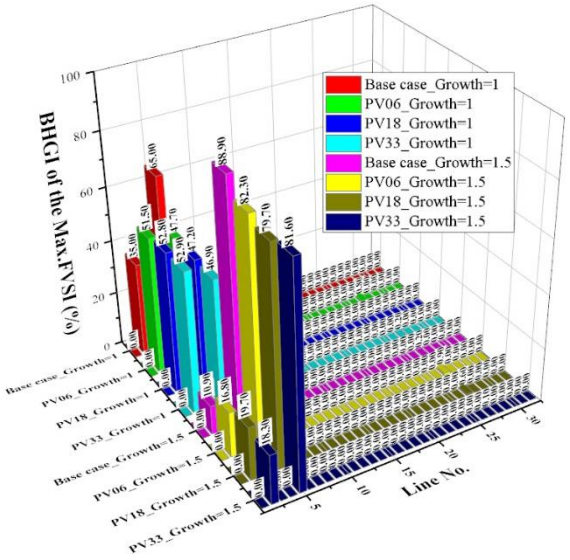

Fig. 4. A percentage of BHGI results for the maximum value of the FVSI.

Fig.5 shows the total real power loss from the MCS process, the impact of the uncertainty load and the growth rate is increased the total real power loss of the grids. Significantly, the growth rate of 1.5 of the loads which are presented by the red colour contour of the high level of the total loss of the electrical power system. The optimal position of the PVSE was revealed by reducing the total power loss of the grids under the growth rate of 1.5. Therefore, the PVSE installation in the grid can be improved the uncertain loss from growth rate but needs to be provided in the optimal sizing and location.

Table 1 illustrates the total power loss of the grid, the maximum, minimum, mean and median were selected to compare each case. The growth rate of 1 of the load revealed the maximum of the real power loss in case 3(PV18_Growth=1) of 340.40 kW and presented the minimum mean value in case 4 (PV33_Growth=1) of 158.64 kW. Meanwhile, the growth rate of 1.5 of the loads revealed the maximum real power loss in case 8 (PV33_Growth=1.5) of 1,270.40 kW and presented the minimum of mean value in case 4 (PV33_Growth=1.5) of 704.02 kW. Therefore, the median values of the total real power loss revealed the installed PVSE, it can be reduced the total real power loss of the grid.

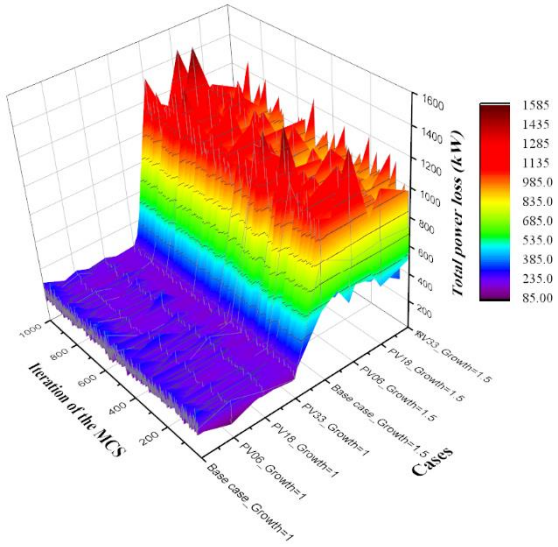

Fig. 5. Total real power loss of each iteration and case.

Table 1. The total real power loss of the test cases

Case	The total real power loss			
	Max.	Min	Mean	Median
	(kW)	(kW)	(kW)	(kW)
Base	348.40	122.90	217.96	214.85
PV06_Growth=1	330.10	86.90	177.35	174.30
PV18_Growth=1	**340.40**	86.10	178.00	174.25
PV33_Growth=1	270.30	87.50	**158.64**	156.30
Base	1,580.60	373.60	847.70	835.95
PV06_Growth=1.5	1,561.40	385.40	754.82	732.65
PV18_Growth=1.5	1,294.90	301.60	706.65	689.65
PV33_Growth=1.5	**1,270.40**	320.00	**704.02**	685.85

Table 2 presents the energy demand of the grid, the uncertainty load revealed the variation of the energy demand. The energy produced from the PVSE location showed the difference in the energy demand related to the total loss of the grid. On the other hand, the growth rate of the loads presented an increase in the energy demand and needed to be managed in optimal condition. In conditions of growth rate equal, one are revealed to the maximum energy demand on the case the installed PVSE on bus No.06 of 4,760.63 kW. Meanwhile, the maximum average value of the energy demand is presented by the base case of 3,927.16 kW. Interestingly, the condition of growth rate equal 1.5 is expressed by the installed PVSE that can reduce the grid's energy demand. Therefore, the location of the PVSE can be improved and reduced the uncertainty load of grids. The PVSE needed to install in an optimal condition and relevant to the energy demand.

Fig. 6 shows the voltage magnitude profiles of the grids, and the voltage profiles are represented by the contouring of each iteration from the MCS simulation. These voltage profile results are represented by the growth rate of 1 and the installation of PVSE. The PVSE are selected to install on buses No.06, 18 and 33. The comparison of voltage profiles are revealed to the voltage level of the grids from the uncertainty load and installed the PVSE. The impact of the uncertainty load are presented by un-predictive and related to the mean and standard deviation of the loads.

Table 2. The energy demand of the test cases

Case	The energy demand			
	Max.	Min	Mean	Median
	(kW)	(kW)	(kW)	(kW)
Base case Growth	4,636.	3,281.	3,927.	3,930.
PV06_Growth=1	4,760.	3,072.	3,900.	3,896.
PV18_Growth=1	4,689.	3,086.	3,893.	3,895.
PV33_Growth=1	4,515.	3,214.	3,875.	3,880.
Base	8,045.	4,899.	6,426.	6,413.
PV06_Growth=1.	7,951.	5,237.	6,332.	6,313.
PV18_Growth=1.	7,561.	5,024.	6,284.	6,278.
PV33_Growth=1.	7,577.	5,132.	6,276.	6,268.

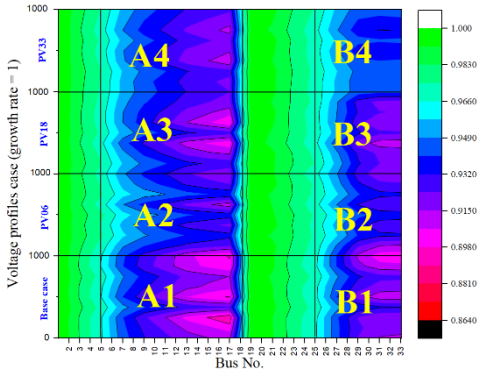

Fig.6 Voltage profiles of each iteration and cases (Growth rate =1)

However, it can be found that the weak point of the voltage profiles (red colour) of the grid is under uncertainty load.

The easy way to analyze the voltage magnitude profiles under contour conditions of the network is defined by a grid with the text Ax, Bx that is used to verify the difference of the voltage profiles case. Therefore, the voltage profiles of each case can be compared by the base case (A1, B1). The impact of voltage profiles is considered by contouring the region that can increase the voltage levels of the grids from the installed PVSE. Therefore, the regions of A2-A4, B2-B4 are voltage improved by the PVSE.

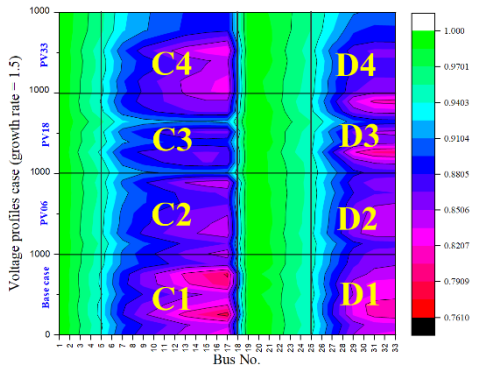

Fig. 7. Voltage profiles of each iteration and cases (Growth rate =1.5).

Fig.7 shows the voltage magnitude profiles of the grids from the MCS, the impact of the uncertainty load and growth rate of 1.5 are presented by the red colour contour revealed the weakness of the voltage profiles on the bus No.13 to No.18 and the end of the root node (bus No.29-33). The grid of voltage profiles with the text Cx, Dx used to verify the difference of the voltage profiles case is the same as previous of the growth rate. Therefore, the installed PVSE can be improved the voltage magnitude profiles when installed by nearly weak points of the voltage profiles on C2-C4 and D2-D4. Experimental results reveal the method offers performance advantages of the installed PVSE and indicate a difference in the voltage profiles contour from the PVSE location. Alternatively, multi-installation of the PVSE can reduce the weak point and increase the grids' voltage profiles level. Therefore, the uncertainty loads and installed PVSE are presented by considering the mean and median values of the voltage magnitude profiles in Table 3.

Table 3. Summary of voltage magnitude profiles

Case	Voltage magnitude profiles of each			
	Max. (p.u.)	Min (p.u.)	Mean (p.u.)	Media (p.u.)
Base	1.000	0.870	0.947	0.939
PV06 Growth=	1.000	0.880	0.953	0.947
PV18 Growth=	1.000	0.864	0.953	0.947
PV33 Growth=	1.000	0.884	0.955	0.950
Basecase Growt	1.000	0.761	0.898	0.884
PV06 Growth=	1.000	0.762	0.905	0.894
PV18 Growth=	1.000	0.786	0.913	0.901
PV33 Growth=	1.000	0.765	0.908	0.896

Table 3 shows the voltage magnitude level from the MCS. The minimum voltage magnitude level is presented in growth rate equal 1.5 on the base case of 0.761 p.u.. Meanwhile, in the condition of installed PVSE are presented minimum voltage profiles on bus No.6 of 0.762 p.u.. However, the mean values of voltage magnitude in all cases can be improved by installing the PVSE that is related to the median value of the variation of the results from the MCS.

The FVSI of the MCS revealed the impact of the uncertainty loads variation of the microgrids. Therefore, the uncertainty loads variation need to be solved when considering the static power flow analysis to determine the level of the load change and voltage collapse of the transmission line. The total real power loss of the grid was varied from the growth rate of the loads and uncertainty load factor. The PVSE can be improved voltage collapse of the transmission line and grids but is needed to find optimal conditions.

5. CONCLUSION

This analysis leads to some useful conclusions, the most important of which is integrated by uncertainty load and the PVSE to the microgrids and using the FVSI condition to find the weak points of the transmission lines. The NPFA was adapted to solve the probabilistic load flow (PLF) with the MCS. It was found that the weak point of voltage collapse was in transmission lines No.2 and No.5 when the BHGI of the FVSI was considered. Interestingly, the growth rates of the loads directly affected the FVSI. Meanwhile, the PVSE integrated into the grid could improve voltage profiles and reduce total real power loss and energy demand based on location. The power system stability can be presented, and the safety margin of the grid increases. Therefore, the PVSE and the impact of uncertainty load need to be managed in the optimal condition. The optimization techniques will be presented in the next study of the VSA for the microgrids system.

REFERENCES

[1] Rojanaworahiran, K.; and Chayakulkheeree, K. 2021. Probabilistic Optimal Power Flow Considering Load and Solar Power Uncertainties Using Particle Swarm Optimization. *GMSARN International Journal* 15 (1): 37-43.

[2] Jung, S.; and Kim, D. 2017. Pareto-Efficient Capacity Planning for Residential Photovoltaic Generation and Energy Storage with Demand-Side Load Management. *Energies* 10 (4): 426-446.

[3] Chen, J. J.; and Wu, Q. H. 2016. Probability interval optimization for optimal power flow considering wind power integrated. In *Proceedings of 2016 International Conference on Probabilistic Methods Applied to Power Systems (PMAPS).* Beijing, China, 16-20 October.

[4] Wang, H.; Xu, X.; Yan, Z.; Yang, Z.; Feng, N.; and Cui, Y. 2016. Probabilistic static voltage stability analysis considering the correlation of wind power. In *Proceedings of 2016 International Conference on Probabilistic Methods Applied to Power Systems (PMAPS).*Beijing, China, 16-20 October.

[5] Ruiz-Rodríguez, F.; Hernández, J.; and Jurado, F. 2017. Probabilistic Load-Flow Analysis of Biomass-Fuelled Gas Engines with Electrical Vehicles in Distribution Systems. *Energies* 10 (10): 1536.

[6] Olivella-Rosell, P.; Villafafila-Robles, R.; Sumper, A.; and Bergas-Jané, J. 2015. Probabilistic Agent-Based Model of Electric Vehicle Charging Demand to Analyse the Impact on Distribution Networks. *Energies* 8 (5): 4160-4187.

[7] Modarresi, J.; Gholipour, E.; and Khodabakhshian, A. 2016. A comprehensive review of the voltage stability indices. *Renewable and Sustainable Energy Reviews* 63: 1-12.

[8] Ratra, S.; Tiwari, R.; and Niazi, K. R. 2018. Voltage stability assessment in power systems using line voltage stability index. *Computers & Electrical Engineering* 70: 199-211.

[9] Martinez-Velasco, J.; and Guerra, G. 2016. Reliability Analysis of Distribution Systems with Photovoltaic Generation Using a Power Flow Simulator and a Parallel Monte Carlo Approach. Energies 9 (7): 537.

[10] Adebayo, I.; and Sun, Y. 2017. New Performance Indices for Voltage Stability Analysis in a Power System. Energies 10 (12): 2042.

[11] Kongjeen, Y.; Buayai K.; and Kerdchuen, K. 2020. Improving Voltage of Microgrid System Based on VAR Control Strategies by Integrating Solar Power System. In *Proceedings of 2020 International Conference on Power, Energy and Innovations (ICPEI)*. Chiangmai, Thailand, 14-16 October.

[12] Abramowitz, M.; and Stegun, I. A. 1964. Handbook of Mathematical Functions. New York: Dover.

[13] Gruosso, G.; Maffezzoni, P.; Zhang, Z.; and Daniel, L. 2019. Probabilistic load flow methodology for distribution networks including loads uncertainty. *International Journal of Electrical Power & Energy Systems* 106: 392-400.

[14] Kansal, S.; Kumar, V.; and Tyagi, B. 2016. Hybrid approach for optimal placement of multiple DGs of multiple types in distribution networks. *International Journal of Electrical Power & Energy Systems* 75: 226-235.

[15] Kongjeen, Y.; Puritatsopol, A.; Buayai, K.; and Kerdchuen, K. 2021. Optimal Substation Placement for Microgrid Power System Based on Nearly Positioning of Bus on the Free Space Area. *GMSARN International Journal* 15 (4): 345-352.

[16] Kongjeen, Y.; and Bhumkittipich, K. 2018. Impact of Plug-in Electric Vehicles Integrated into Power Distribution System Based on Voltage-Dependent Power Flow Analysis. *Energies* 11 (6): 1571-1587.